 https://doi.org/10.3311/PPci.20187

Periodica Polytechnica Civil Engineering, 67(1), pp. 200–210, 2023

Feasibility of Onboard Smartphones for Railway Track Geometry Estimation: Sensing Capabilities and Characterization

Ákos Vinkó[1*], Tamás Simonek[1], Csaba Ágh[2], Attila Csikós[1], Balázs Figura[2]

[1] Department of Highway and Railway Engineering, Faculty of Civil Engineering, Budapest University of Technology and Economics, Műegyetem rkp. 3, H-1111 Budapest, Hungary
[2] MÁV Central Rail and Track Inspection Ltd, Péceli u. 2., H-1097 Budapest, Hungary
[*] Corresponding author, e-mail: vinko.akos@emk.bme.hu

Received: 20 March 2022, Accepted: 23 October 2022, Published online: 21 November 2022

Abstract

The performance and sensitivity of smartphone sensors developed rapidly in recent years. Due to their accessibility and low costs compared to other industrial solutions, the use of smartphone sensors has become more and more common. In this article, the validity and reliability of a smartphone application in railway track geometry estimation are tested on a conventional rail line. This work focused on Galaxy S-series smartphones of Samsung and proposes an evaluation of the onboard sensing capabilities of their inertial sensors with the comparison of synchronous measurements by a multi-functional Track Recording Vehicle equipped with a contactless Track Geometry- (TGMS), and a Vehicle Dynamic Measuring System (VDMS). The raw accelerometer recordings showed a high-degree correlation with VDMS in both signal magnitude and waveform. The accuracy of gyroscope angular tracking in heading and pitching angle calculation was in the range of 0.2°–0.6°, which allowed the acceptable estimation of the central angle and the radius of horizontal curves. Based on the kinematic analysis techniques, the roll flexibility coefficient of the vehicle was determined, which allowed calculating the cross-level and the twist of the track. Furthermore, the local extreme values of the roll-rate gyro correlate with the isolated track geometry defects of the track twist gathered by TRV's TGMS. Despite its limitations, the application of smartphones represents a prospective technological opportunity to explore new approaches and support rail asset management.

Keywords

track geometry estimation, track recording car, in-service vehicle, Inertial Measurement Unit (IMU), smartphone

1 Introduction

Infrastructure managers are responsible for the assurance of reliable rail infrastructure that meets the needs of the safe and cost-efficient operation of the rail services. In modern rail asset management, the Internet of Things-based life cycle maintenance strategy integrates the data from track recording cars and visual as well as other track inspections. With extensive and frequent measurements, this method makes it possible to detect the track irregularities in their early stage. The timely maintenance can increase the railway operation's reliability and minimize the railway infrastructure's long-term cost.

In Hungary, on railway lines belonging to Hungarian State Railways (MÁV), objective measurements are performed by track recording cars. The track inspection is performed twice or three times per year, depending on the line category. The temporary changes in traffic volume, axle loads, or environmental conditions may rapidly increase track deterioration. Still, the high costs of track recording cars and rail traffic management limit the maximal frequency of track inspections. The time interval between inspections can be reduced by performing measurements with in-service vehicles. In-service vehicles with built-in measurement systems are already used in many countries for track condition monitoring [1–4]. These systems usually use inertial sensors to indirectly estimate the track condition based on the measured irregular vehicle motion.

Smartphones developed rapidly in recent years. Nowadays, most middle-end smartphones have built-in accelerometer and gyroscope. The improvement in the capabilities of these sensors (sensitivity, measurement range, offset accuracy, and noise density) opens up the possibility of their use in railway diagnostics. Onboard smartphones could provide a cost-effective method to

Cite this article as: Vinkó, Á., Simonek, T., Ágh, C., Csikós, A., Figura, B. "Feasibility of Onboard Smartphones for Railway Track Geometry Estimation: Sensing Capabilities and Characterization", Periodica Polytechnica Civil Engineering, 67(1), pp. 200–210, 2023. https://doi.org/10.3311/PPci.20187

complement the assessment of the structural performance and dynamic response of vehicle-track interaction with the ability to increase the number of measurements without disturbing rail traffic.

There is an increasing number of studies investigating the possibility of using smartphones to measure ride comfort [5–9] or evaluate track quality [10, 11]. However, only a few ongoing projects have aimed to estimate track geometry parameters [12, 13].

This paper intends to examine the possible use of smartphones in railway track geometry inspection by performing synchronous measurements with a certified multi-functional Track Recording Vehicle (TRV). The data provided by TRV and smartphone measurements are compared to determine the achievable accuracy and sensing capabilities of smartphone inertial sensors. The following section gives details about the investigated rail line and the newly developed android platform-based data acquisition. Section 3 introduces the measurement setup and the applied data processing methods. Then, Section 4 summarizes the line test results and gives the main conclusions

2 Investigated rail line

The measurements were performed on railway line No. 2 in Hungary, between the stations of Rákosrendező and Esztergom. The railway line was recently renovated between 2012 and 2015. The line lies in a hilly region that results in its alignment containing many small radius curves and a wide range of gradients. The "extreme" values of alignment parameters (compared to most Hungarian railway lines) provide an opportunity to examine the accuracy of the smartphone inertial sensors in a wide range of situations.

The sensor data of smartphones was recorded at the highest possible sampling rate using the developed "CAFat" Android mobile app, which is capable of time-synchronized recording of all phone sensor data and GPS location information. Two middle-end smartphones were used for the measurements, a Samsung Galaxy S6 and a Samsung Galaxy S10.

The smartphone measurements were compared to the data of the multi-functional track recording vehicle having a contactless, chord-offset based Track Geometry Measuring System (TGMS) synchronized with a Vehicle Dynamic Measuring System (VDMS) consisting of 24 accelerometers mounted on different structural parts of the vehicle [14]. The results of the VDMS depend on the velocity of the vehicle, so the results were considered reliable only when the velocity was higher than 40 km/h. Most of the examinations were carried out on a section near the station of Pilisvörösvár, consisting of two small radius curves with transition curves (a right and a left reverse curve with the radius of $R_{1,2}$ = 250 m, see Fig. 1), but some parameters were further examined on multiple different locations.

3 Methodology

The raw acceleration time histories of the smartphones were validated by the TRV's VDMS. At the same time, the accuracy of estimated track geometry and alignment parameters was determined by evaluating the relative deviation from TRV's TGMS and nominal design values.

3.1 Measurement setup

For the simultaneous measurements, smartphones were placed in the track observation room of the TRV, close to

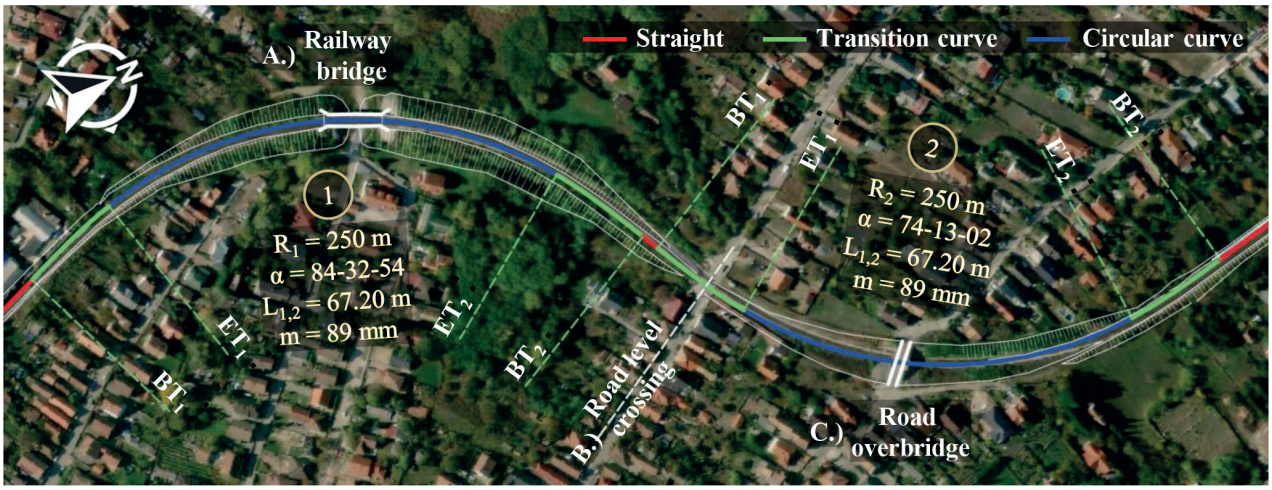

Fig. 1 Aerial view (Bing Maps) of the examined track section, highlighting the track alignment parameters and important structures along the track (Railway line No. 2, Budapest - Esztergom, Hungary)

the floor-mounted sensors TRV1 and TRV2 of VDMS [15]. The S6 and S10 smartphones were mounted to the window glasses above TRV1 and TRV2, respectively (Fig. 2). A thin silicone pad fixed the phones to prevent any relative movements. The standard right-handed relative coordinate system of a smartphone can be seen in Fig. 3.

The smartphone-based coordinate system was transformed to use the traditional terminology (x: longitudinal track axis, y: lateral axis, z: vertical axis). The motion data from the accelerometer and gyroscope in the S6 and S10 smartphones was collected at 200 Hz and 500 Hz sampling rates, respectively. TRV1 is a single-axis accelerometer sensing only in the vertical direction, while the TRV2 sensor set includes two single-axis accelerometers assembled and senses in vertical and lateral directions at the sampling rate of 300 Hz. However, the TRV's VDMS filters out frequencies higher than 16 Hz.

3.2 Data pre-processing for correlation analysis

The raw acceleration data of phones were low-pass filtered with a 16 Hz cut-off frequency to be comparable to VDMS. The smartphone's filtered acceleration data was validated by its time history-based comparison with the reference sensor data (TRV1 and TRV2) of the TRV's VDMS (Section 4.1). The starting timestamps of the smartphones and the TRV were synchronized after the measurement using their internal clocks.

The acceleration stationary base drift over time in both measurement systems was corrected by subtracting the mean of time domain data. Furthermore, a Simple Moving Average (SMA) was also applied to figurative representation. The optimal time window size for the SMA was determined by comparing the Sum of Absolute Differences

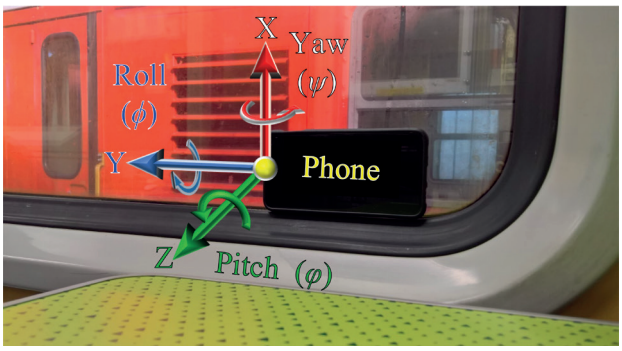

Fig. 3 The Samsung Galaxy S6 smartphone mounted to the window glass and the applied relative coordinate system. Axis conversion: X→z (vertical), Y→x (longitudinal), Z→y (lateral) direction

(SAD) of the raw data and the SMA data series for different window sizes. The time criterion started with 2 s width time windows, and 0.1 s have progressively narrowed them until no substantial additional information in the time domain was obtained. The difference in neighboring SAD values was the lowest between the window sizes of 0.7 s and 1.2 s. The applied window size was set to be the mean of these values and was decided to be 1 s.

3.3 Estimation of the track alignment and track geometry parameters

Window glass-mounted smartphones in TRV can measure the regular and irregular motions of the carbody. After further processing with the consideration of vehicle characteristics, the parameters of the track alignment can be estimated. Since railway line No. 2 was renovated recently, the track alignment probably accurately matches the design values. The margin of error can be calculated by examining the difference between the design and measured values.

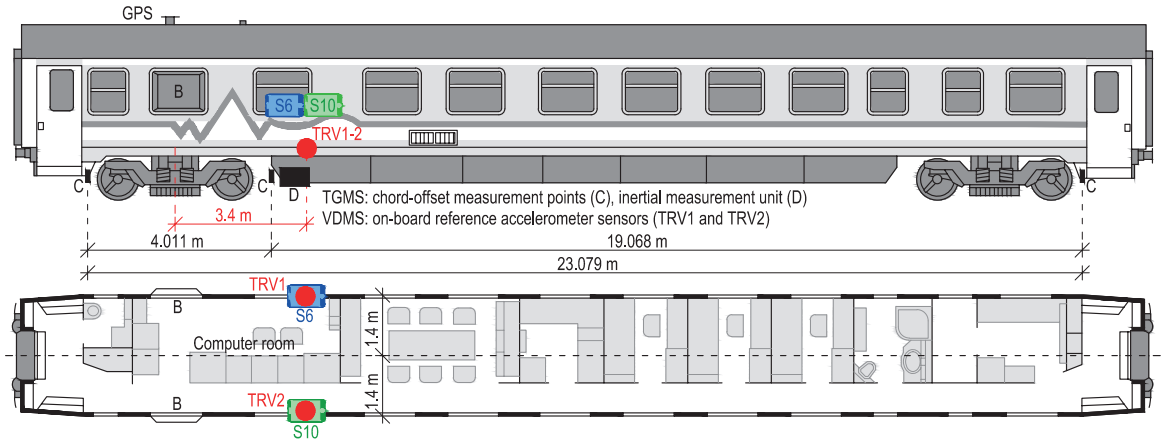

Fig. 2 Experimental setup of the window glass mounted Samsung Galaxy S6 and S10 smartphones in the two-functional Track Recording Vehicle (TRV) with the indication of the elements of TRV's sub-systems relevant for comparison: the contactless, optical Track Geometry Measuring System (TGMS) and the Vehicle Dynamic Measuring System (VDMS) including the sub-set of accelerometer sensors (TRV1 and TRV2)

From the 3-axial acceleration and angular velocity data of the smartphones (Fig. 3), the non-compensated lateral acceleration, the yaw-rate $\dot{\psi}(t)$, and the roll-rate $\dot{\varphi}(t)$ orientation data were used to estimate the alignment parameters. As the parameters mentioned above differ in nature, different methods were used for preprocessing. Gyroscope data was filtered by an elliptic (Cauer) 0.005–2 Hz bandpass filter to remove the effect of the gyro drift and the noise not relevant to irregular carbody oscillations caused by track irregularity. The upper limit of the bandpass filter matches the recommended value of standard EN 12299 [16]. Parameters for filtering noise out of accelerometer records were set concerning a sensor fusion approach.

The examined parameters included the *track curvature*, the *carbody heading* (yawing), *tilting* (rolling) and *pitching angle*, and their *rate of change*. The following methods were used to calculate these parameters in the time domain.

3.3.1 Estimation of heading angle and curvature

In the case of conventional vehicles with pivoting bogie concept, the heading angle differences calculated between the preceding and following straight sections reliably characterize the central angles of the horizontal curves. The heading angle can be determined by cumulative trapezoidal integration of the bandpass-filtered rotation around the vertical axis ($\dot{\psi}_{bpf}(t)$) in time domain using Eq. (1).

$$\psi(t) = \frac{1}{2}\sum_{n=1}^{N}(t_{n+1} - t_n)\left[\dot{\psi}_{bpf}(t_n) + \dot{\psi}_{bpf}(t_{n+1})\right], \tag{1}$$

where $(t_{n+1} - t_n)$ is the time spacing in the unit of [s] between each consecutive pair of points; $\dot{\psi}_{bpf}(t)$ is the bandpass filtered heading (yawing) rate [rad/s].

The horizontal curvature G in the unit of [1/m] can be calculated from the bandpass-filtered yaw-rate gyro $\dot{\psi}_{bpf}$ and the vehicle velocity v [m/s] using Eq. (2):

$$G(t) = \frac{\dot{\psi}_{bpf}(t)}{v(t)}. \tag{2}$$

3.3.2 Estimation of track cant

In the case of vehicles with a torsionally stiff body, the quasi-static value of *track cant* ($\acute{s}$) can be reliably estimated from the tilting angle ϕ [rad] of the carbody. Quasi-static cant represents the smoothed value (design value) of cant. The carbody does not follow the minor distortions of the track accurately. Therefore, high-frequency components of cant cannot be calculated from carbody movements. Based on the denominations of Fig. 4, the measured lateral carbody acceleration $a_{y,lpf}$ [m/s^2], which is smoothed with 5 Hz low-pass filter, can be considered as

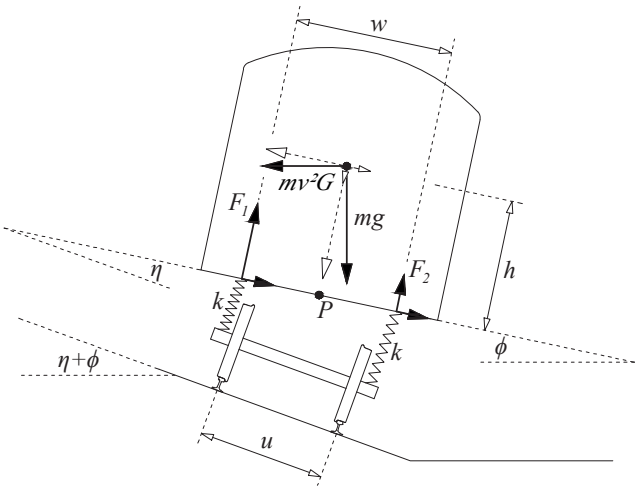

Fig. 4 Track cant estimation from carbody tilting: considering conventional passenger coach

$$a_{y,lpf}(t) = v^2(t)\cdot G(t)\cos\phi(\mathrm{t}) - g\cdot\sin\phi(t). \tag{3}$$

Substituting Eq. (2) into Eq. (3) and using small-angle approximations $\cos\phi \approx 1$ and $\sin\phi \approx \phi$, for carbody tilting angle yields:

$$\phi(t) = \frac{v\cdot\dot{\psi}_{bpf}(t) - a_{y,lpf}}{g}. \tag{4}$$

However, the tilting angle of carbody (ϕ) and the track cant angle (δ) is equal only if the train's speed is the equilibrium speed. In any other case, there is a cant deficiency or cant excess. Therefore, the carbody flexibility should be considered as mentioned in Point 5.2 of standard EN 15273-1 [17]. A torque equilibrium equation (Eq. 5) about point P (Fig. 4) was investigated as follows:

$$(F_1 - F_2)\cdot\frac{w}{2} + h\cdot m\cdot g\sin\phi - h\cdot m\cdot v^2 G\cdot\cos\phi = 0, \tag{5}$$

where F_1 and F_2 [N] are the magnitudes and w [m] is the distance of vertical components of the forces acting on carbody from the bogie, h [m] is the distance of point P from the centre of gravity of the carbody, m [kg] is the relevant mass of carbody.

Substituting Eq. (3) into Eq. (5), yields:

$$(F_1 - F_2)\cdot\frac{w}{2} = h\cdot m\cdot a_{y,lpf}. \tag{6}$$

Using Hooke's law, the angle difference η between carbody and track cant is determined by asymmetrical compression as

$$\eta = \frac{F_1 - F_2}{wk}, \tag{7}$$

where k [N/m] is the equivalent stiffness of the primary and secondary suspension. Hence, quasi-static track cant $\hat{s}$ in the unit of meter can be calculated with the help of Eqs. (4), (6) and (7) as

$$\hat{s} = (\phi + \eta) \cdot u = \frac{u}{g}\left(v \cdot \dot{\psi}_{bpf} + c \cdot a_{y,lpf}\right), \tag{8}$$

where u is the distance between the points of contact of the mean wheel circles with the rails (u = 1.500 m) and c is a dimensionless constant because it depends only on the vehicle characteristics:

$$c = \frac{2 \cdot g \cdot h \cdot m}{w^2 k} - 1 . \tag{9}$$

Value of c was simply obtained using Eq. (8) by means of iteration on the basis of known cant data s of curves on the test track. The value of c = 0.8 was found to be universal for the roll flexibility of the investigated vehicle. If c is already known for a vehicle, the quasi-static cant of unknown curves can be measured using Eq. (8).

3.3.3 Estimation of track twist

Track twist is defined as the variation in actual track cant between two locations, separated by a nominated distance (base) along the track. Quasi-static value of track twist can be reliably estimated on any base-length. The quasi-static twist represents the smoothed value (e.g., gradient value of a cant transition ramp) of the twist. The carbody does not follow the minor distortions of the track accurately. Therefore, high-frequency components of twist cannot be calculated from carbody movements. However, severe track twist defects can be detected due to the post-shock and self-excited oscillation of carbody. Two different methods were developed for twist estimation: calculation from the track cant ($\hat{s}$) determined by Eq. (8) taking derivative by convolution according to Eqs. (10) and (11), or directly from the measured roll-rate gyro data of the vehicle, according to Eq. (12). The relationship between the estimated track twist and the angular velocity of the tilting (rolling) motion is illustrated on Fig. 5.

$$Twist_b(t) = \sum_j Q(j) \cdot \hat{s}(t - j) , \tag{10}$$

$$Q = \left[\underbrace{0\ 0\ \ldots\ 0}_{\frac{b}{v(t)} \cdot Fs}\ 1\ \underbrace{0\ 0\ \ldots\ 0}_{\frac{b}{v(t)} \cdot Fs}\ -1 \right], \tag{11}$$

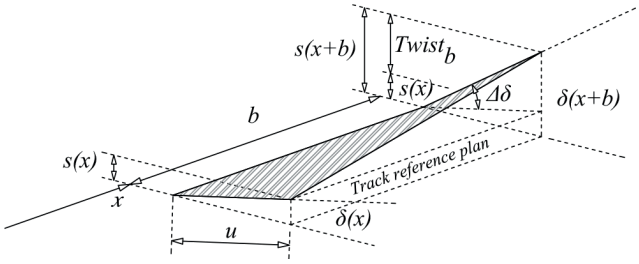

Fig. 5 The calculation principle of track twist indicating the track cant angle and its rate of change on the nominated distance (b)

$$Twist_b(t) = \frac{u \cdot b}{v(t)} \dot{\phi}_{bpf}(t) , \tag{12}$$

where u = 1.500 m; x [m] is the spatial distance along the track; Q is the convolution kernel; j is the number of convolution kernel elements; δ [rad] is the track cant angle; b [m] is the applied twist base length; Fs [samples/s] is the phone sample rate; $v(t)$ [m/s] is the vehicle velocity; $\dot{\psi}$ [rad/s] is the yaw-rate gyro data; $\dot{\phi}$ [rad/s] is the roll-rate gyro data; s is the real while $\hat{s}$ is the estimated cant value in [m].

4 Comparison and characterization

4.1 Validation of smartphone Raw Sensor Data

Even though TRV's TGMS includes a carbody-mounted 6 DoF IMU (Inertial Measurement Unit), only the acceleration data of smartphones could be validated by comparison with the TRV1 and TRV2 of VDMS, as the raw gyroscope recordings of TGMS was not available in TRV's sensor log.

The raw data recorded on the track section illustrated in Fig. 1 was examined on the basis of both time and frequency domains. Correlation analysis was used for the time-series (Fig. 6) and normalized Fourier Amplitude Spectrum (FAS) for the frequency domain-based comparisons (Fig. 7).

The sampling rate of the VDMS's accelerometer sensors (≈300 Hz) is between the data acquisition capabilities of S6 (200 Hz) and S10 (500 Hz) phones. Besides, the smartphones provide the measurement results on all available frequencies, but the TRV's VDMS filters out the frequencies higher than 16 Hz. In Fig. 7, the FAS graphs of TRV1-2 and phones clearly demonstrate these differences in the frequency components. Motion tracking via S6 and S10 smartphones were compared in the time domain to the selected reference accelerometers of VDMS. The vertical and lateral acceleration of TRV2 (at the same section as the S10 smartphone) is displayed with the simultaneously recorded smartphone data in Fig. 6. Phone data displayed as raw are the result of the same 16 Hz low-pass filter used in VDMS. On the examined track section, locally poor track

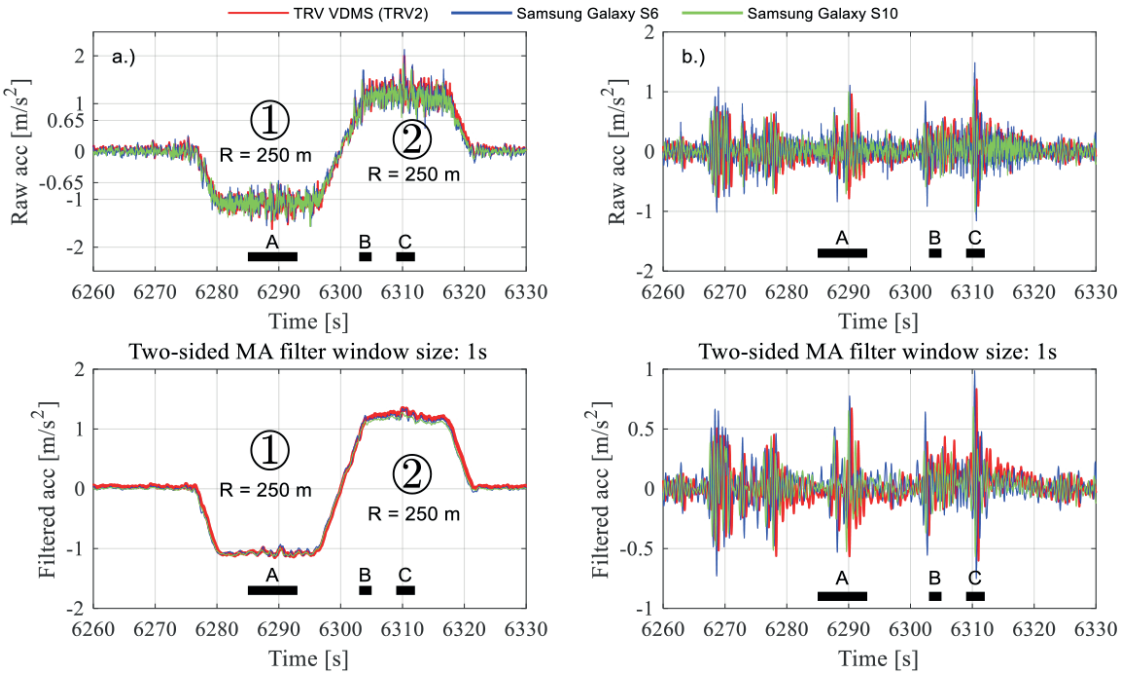

Fig. 6 Time domain representation of the smartphones (Samsung Galaxy S6, Samsung Galaxy S10) and the VDMS (TRV2) accelerometer data; a) lateral acceleration; b) vertical acceleration (A, B and C signs represents the structures along the track according to Fig. 1)

geometry can be observed at railway structures, which are marked in Fig. 6 as follows: "A" railway bridge, "B" road level crossing, "C" road overbridge. Local extreme values can be seen at these structures, especially on the graphs of the vertical accelerations (Fig. 6(b)). Pearson's Correlation Coefficient was used to measure the closeness of the relationship between them.

The correlation was calculated per sensing axis, separately for the lateral and vertical acceleration components (Fig. 7). Since the TRV1 is a single-axis accelerometer sensing only in the vertical direction, the lateral acceleration of the S6 phone was compared to TRV2. The correlation of the lateral acceleration is above 95% in the case of both smartphones, the correlation of the S10 phone even exceeds 99%. The correlation of the vertical acceleration is similarly high in the case of the S10 phone, above 90%, but the correlation of the S6 is lower (81%).

For positioning, the smartphones use Global Navigation Satellite System (GNSS) solutions operating mainly in single-point position mode and estimate velocity by differencing two consecutive positions. In contrast, the TRV uses an axle-mounted odometer sensor to determine the pulses per revolution. The smartphone's positioning precision (the maximal distance of the measured position from the real one) varied in a wide range. Analyzing the data of multiple measurements showed that the average positioning precision of the older S6 smartphone was 7.3 m, and the standard deviation was 2.8 m. The newer S10 produced significantly better results, the average accuracy was 4.9 m, and the standard deviation was 1.4 m. The range of position accuracy changed between 3 and 48 m for the S6, and between 2 and 12 m for the S10. The GNSS-based velocity estimation accuracy changed according to satellite broadcast signal quality. The changes were probably caused by the topography and the atmospheric conditions [18]. On the investigated rail line, a hilly region was compared to a plain terrain region to examine the effect of the terrain conditions. The data series of both sections included around 100 000 data points. The average difference between the real and the estimated velocity on the hilly region was 1.58 km/h, and the standard deviation was 1.44 km/h. On the plain section, the average difference was 0.90 km/h, and its standard deviation was 0.63 km/h. The required reliability cannot be ensured during the measurements because of the masking effect of the carbody (metal-coated window glasses) and the local signal degradation in the harsh environments (deep cutting, combined section with cutting and embankment, as well as the tree foliage) together can cause both the position and velocity data to be locally inaccurate or unusable. Therefore, the TRV velocity data (synchronized with the smartphone measurement data) was used in later examinations.

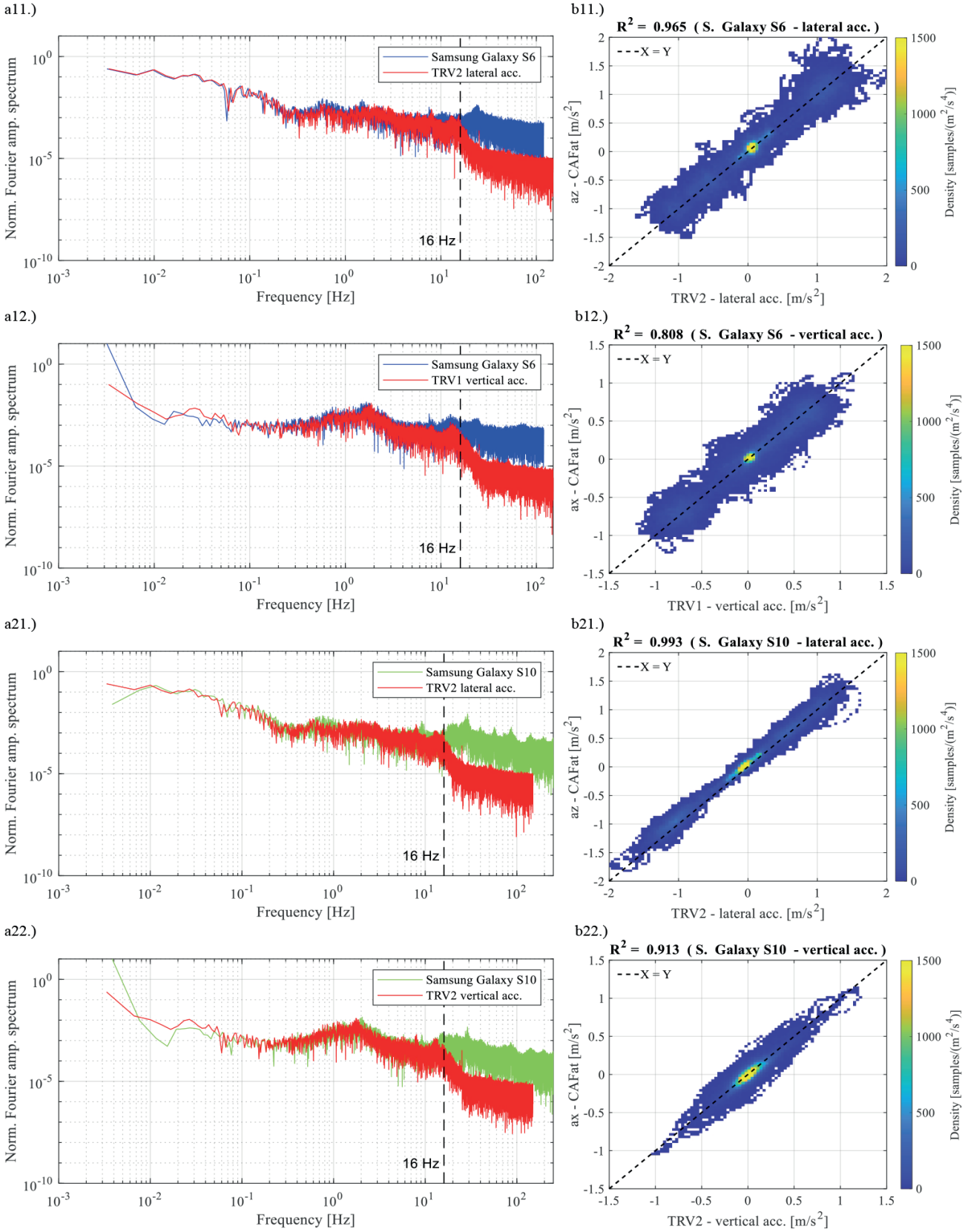

Fig. 7 Time and frequency domain representation of the acceleration data simultaneously recorded by both smartphones and VDMS (TRV1 and TRV2) along the track according to Fig. 1.; a) Normalized Fourier Amplitude Spectrums, b) Binned scatter plot representation of correlation per sensing axis

4.2 Validation of the estimated alignment parameters

First, the calculated heading and pitching angles were compared to the design values of the track's horizontal and vertical layouts. Even though the design values of horizontal curves vary over a wide range, their investigation showed (Table 1) that the central angle can be estimated with an accuracy of a few tenths of a degree. In most cases, the relative error was lower than 1%. From the point of view of track alignment design, changes in the vertical alignment are usually in a lower order of magnitude than the ones of the horizontal alignment.

In the case of horizontal alignment, where the central angle of curves varies in a range of around 6 to 90°, smartphones can measure the central angle of a curve with an accuracy of a few tenths of a degree (Fig. 8). If same relative accuracy is considered in all sensing directions, smartphones should be able to detect a change in the longitudional gradient larger than 10‰.

Considering the relative accuracy, the selected vertical points of intersections for precision tests had a relatively significant change in gradient, between 10 and 15‰ (Table 2). The results confirmed that the absolute accuracy in this smaller range of angles is similar to the larger ranges, a few tenths of a degree. With this level of accuracy, larger changes in the gradient can be detected, and their magnitude can be estimated.

The second investigated parameter was the track horizontal curvature, which can be calculated from the yaw-rate gyro and the vehicle velocity using Eq. (2). As the results in Table 1 show, smartphones can measure the angular velocity relatively accurately, but the GNSS-based velocity estimation sometimes produces false results, due to the reasons detailed in Section 4.1. Therefore, instead of phone GNSS measurements, the synchronized velocity of TRV was used to characterize the maximum achievable accuracy of the phone's built-in gyroscope. The results are displayed in Fig. 8 and in Table 3, where the design values of the radii are corrected with the distance of the smartphone's position relative to the track centerline. The calculated value of the radius is more accurate in small radius curves and becomes less accurate as the radius increases. The accuracy of the Galaxy S10 smartphone stayed below 1% even in the case of the 1100 m radius curve, which was the largest among the examined curves.

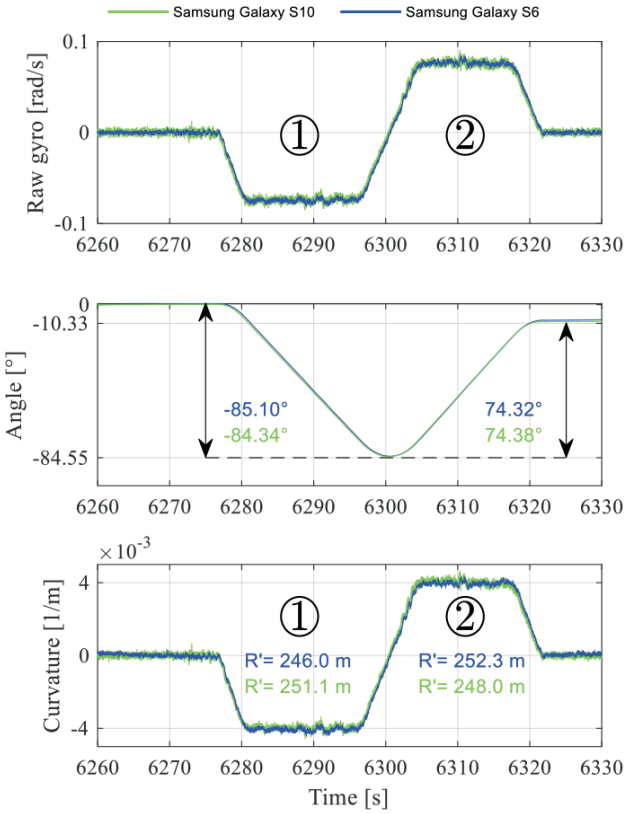

Fig. 8 The central angle and curvature calculated from the raw gyro data on the examined track section illustrated in Fig. 1

Table 1 The design and estimated values of the central angles (S6, S10)

Radius [m]	Central angle Design value [°]	Relative error Samsung G. S6 [°] [%]	Relative error Samsung G. S10 [°] [%]
250 ①	84.548	0.548° (0.55%)	0.210° (0.25%)
250 ②	74.217	0.103° (0.14%)	0.162° (0.22%)
604.2	60.033	0.051° (0.09%)	0.218° (0.36%)
600	19.395	0.092° (0.47%)	0.164° (0.85%)
1400	6.229	0.073° (1.18%)	0.101° (1.61%)

The horizontal layout of track curves ① and ② is illustrated in Fig. 1

Table 2 The estimated and design values of the change in gradient

Design value [‰]	Design value [°]	Relative error Samsung G. S6 [°] [%]	Relative error Samsung G. S10 [°] [%]
14.1	0.8078	0.036° (4.51%)	0.196° (24.32%)
11.3	0.6474	0.098° (15.18%)	0.043° (6.68%)
11.5	0.6589	0.191° (28.94%)	0.178° (27.06%)

Table 3 The estimated and nominal design values of the curve radii

Design value of curve radii* [m]	Relative error Samsung G. S6		Relative error Samsung G. S10	
	[m]	[%]	[m]	[%]
250 ①	2.6	1.05	0.3	0.12
250 ②	0.9	0.36	0.6	0.24
604.2	3.1	0.51	3.2	0.53
1100	12.2	1.11	6.3	0.57

The horizontal layout of track curves ① and ② is illustrated in Fig. 1
* Nominal radius of curves modified by the width of the vehicle

Fig. 9. displays the curvature, cant, and track twist (on 6 m base-length) measured by the TRV, synchronized with the processed measurement data of the smartphones. In the case of smartphones, the travelled distance was calculated using the velocity data of the TRV after synchronizing the time data of the two measurement systems.

The track cant was estimated based on the compensated tilt of the carbody, which was calculated from the smartphone inertial sensor data and the synchronized TRV velocity data using Eq. 8. The carbody roll is not equal to the track cant, depending on asymmetric spring compression arising from cant deficiency or cant excess. The introduced solution in Section 3.3.2 considers the carbody roll effect by introducing the roll flexibility coefficient (c) of the vehicle suspension. The comparison of the estimated cant to the real cant provided by the TGMS along the track section illustrated in Fig. 1. can be seen in Fig 9(b). Table 4 introduces the relative error of cant values averaged on the circular curve sections with constant superelevation. The average difference is less than 10 mm in all investigated sections.

The algebraic difference between two estimated cant taken at a defined distance apart (Eq. 10.) and the TRV's track twist defined with the same base-length were compared. Exceedance of a limit value (10 mm was investigated. Fig 9(c). shows the track twist (6 m base-length) estimated using Eq. 10. and the TRV data for the same track segment. In the figure, the 10 mm limit is indicated by the grey dashed line, while the limit exceedance in the case of TRV and smartphone-based inspection is marked with red and black colored numbers, respectively. The detailed comparison results of the two systems are listed in Table 5. It can be noticed that the maximum distance deviation of the out-of-limit points from the two systems is less than 10 m. The track twist graphs of both systems contain the baseline shift due to the cant transition and the peak values superimposed on it. Track twist recorded by TRV has eight peak values (marked by red numbers: '1-3', '4', '5', '6', '7', '8' on Fig. 9(c)) larger than 10 mm, of which the smartphone-based system can identify four. Head of

Table 4 The estimated and the TRV recorded values of track cant

TRV average track cant [mm]	Relative error Samsung G. S6		Relative error Samsung G. S10	
	[mm]	[%]	[mm]	[%]
+71.005 ①	+1.437	2.02	+2.783	3.92
-77.762 ②	-4.373	5.62	-1.275	1.64

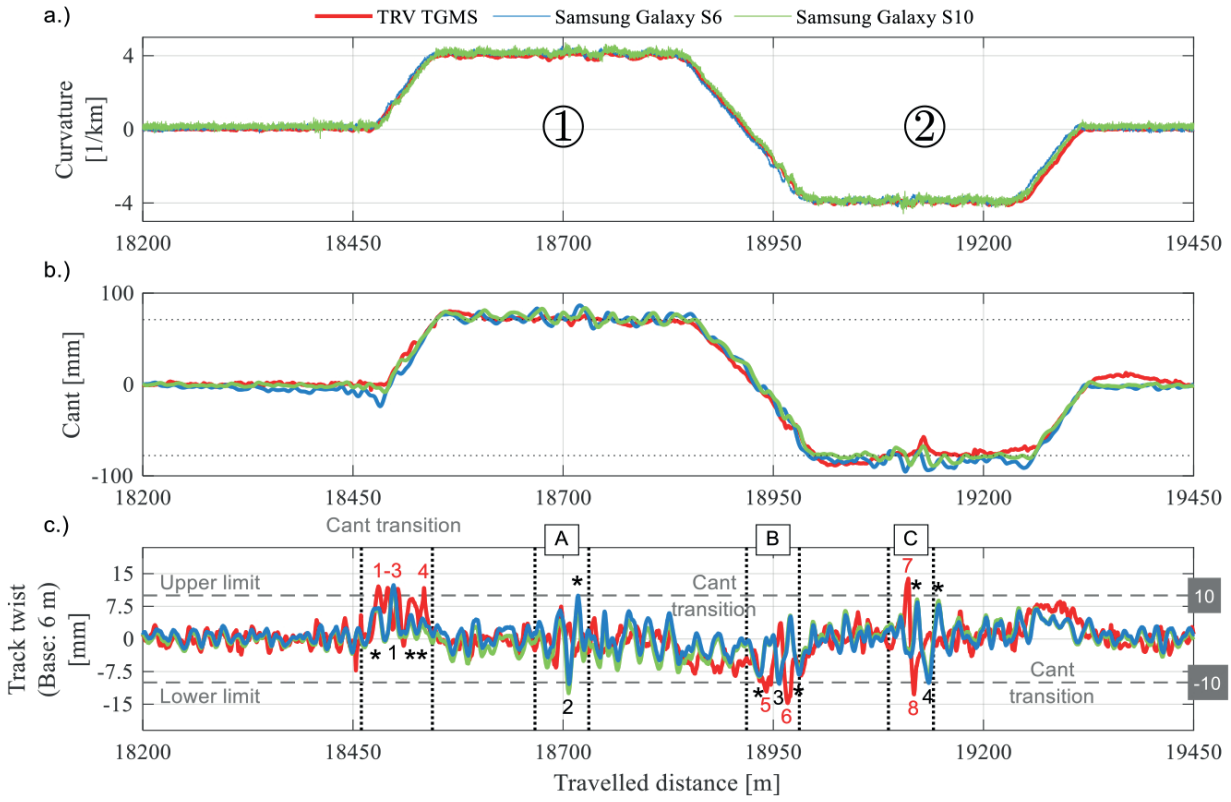

Fig. 9 Results calculated from smartphone sensor data (Samsung Galaxy S6, Samsung Galaxy S10) and compared with track recording car (TRV) results: a) horizontal curvature; b) calculated and measured track cant; c) calculated and measured track twist over 6 m base (A, B and C signs represents the objects along the track according to Fig. 1)

Table 5 The track twist comparison result of the smartphone-based track inspection system and the TRV.TGMS

Deviation points	NO	YES	YES	NO	NO	NO	YES	NO	YES
TRV TGMS	1	2	3	4	-	5	6	7	8
S6 – S10	*	**1**	**1**	*	**2**	*	**3**	*	**4**
Trackside structure	-	-	-	-	A	B	B	C	C
Distance (TRV) [m]	18480.7	18491.5	18503.5	18534.9	-	18941.71	18966.71	19110.71	19117.46
Distance (S10 & S6) [m]	18477.1	18497.0	18497,0	18533.0	18707.1	18932.2	18956.3	19120.4	19127.8
Distance deviation [m]	3.6	-5.5	6.5	2.0	-	9.51	10.41	-9.69	-10.34
Deviation level (TRV)	**11.95**	**11.73**	**11.51**	**11.54**	**-**	**-12.11**	**-14.66**	**13.86**	**-12.75**
Deviation level (S10)	6.46	11.49	11.49	3.22	-12.31	-8.583	-9.985	8.744	-8.928
Deviation level (S6)	7.04	11.51	12.36	4.62	-10.30	-8.372	-10.267	8.353	-10.019

Table 5 shows the existence of peak values detection by S6-S10 smartphones with "YES" or "NO" phrases. In the estimated track twist signal, there are post-"shock" oscillations after the location of isolated defects. This led to severe, sometimes opposite peak values (red colored no. '5'-'6' on Fig. 9(c)) at the same location as TRV.

5 Conclusions

In the proposed onboard inspection solution, smartphone inertial sensors can provide reliable data about carbody dynamics, and are able to detect track sections in poor condition by measuring the damped carbody oscillation on track irregularities.

The raw acceleration data of the smartphones was compared to the TGMS and VDMS of the TRV. Local extreme values were visible at the same locations in the data series of both measurement systems, and the correlation between the smartphone's data and neighboring VDMS sensor data surpassed 90% in the case of the Galaxy S10.

Smartphone gyroscopes can measure yaw-rate and pitch-rate vehicle motion with a few tenths of a degree, which is surprisingly accurate considering their intended use. This level of accuracy makes it possible to detect larger (10–15‰) changes in the gradient. In the case of conventional vehicles with pivoting bogie concept, the central angle of a horizontal curve can be estimated with an error of less than 1%.

The radius, as the reciprocal of the curvature, can be estimated with variable accuracy depending on the range of radius values: curves with a radius less than 600 m can be detected with an accuracy better than 5 m. If differently structured vehicles are used for measurement, it is essential to consider their structural design, geometric properties, and the smartphone's location within the vehicle.

Over- or underbalanced conditions of curving vehicles can be accurately detected with the sensor fusion of the smartphone's accelerometer and the gyroscope. Further-more, if the roll flexibility coefficient index (c) is well defined, the calculated compensation of carbody tilt provides accurate information about track cross-level. The roll-rate motion of carbody can be calculated from the smartphone data by taking the algebraic difference between two compensated carbody tiltings at a defined distance apart. The comparison with the TGMS twist data showed that 'quasi-static' (design) values of cant and twist (e.g., the slope of cant transition ramps) can be estimated reliably. Regarding isolated track twist defects, only severe twists can be consistently detected due to the post-shock and self-excited oscillation of carbody.

The present study does show that high-end smartphones used as onboard devices can effectively complement rail asset management due to the reliable sensitivity of their built-in inertial sensors. This paper also deserves further investigation that will focus on improving the GNSS-based positioning and velocity estimation as well as sensor calibration, including an investigation of external influences on the accuracy of the spatial orientation of smartphones from different brands.

Acknowledgement

The research reported in this paper and carried out at BME has been supported by the NRDI Fund (TKP2020 IES, Grant No. TKP2020 BME-IKA-VIZ) based on the charter of bolster issued by the NRDI Office under the auspices of the Ministry for Innovation and Technology.

References

[1] Yeo, G. J., Weston, P. F., Roberts, C. "The utility of continual monitoring of track geometry from an in-service vehicle", In: 6th IET Conference on Railway Condition Monitoring (RCM 2014), Birmingham, UK, 2014, pp. 1–6. ISBN: 978-1-84919-913-1 https://doi.org/10.1049/cp.2014.0997

[2] Heirich, O., Lehner, A., Robertson, P., Strang, T. "Measurement and analysis of train motion and railway track characteristics with inertial sensors", In: 2011 14th International IEEE Conference on Intelligent Transportation System (ITSC), Washington, DC, USA, 2011, pp. 1995–2000. ISBN: 978-1-4577-2198-4 https://doi.org/10.1109/ITSC.2011.6082908

[3] Boronakhin, A. M., Podgornaya, L. N., Bokhman, E. D., Filipenya, N. S., Filatov, Y. V., Shalymov, R. B., Larionov, D. Y. "MEMS-Based Inertial System for Railway Track Diagnostics", Gyroscopy and Navigation, 2(4), pp. 261–268, 2011. https://doi.org/10.1134/S2075108711040055

[4] Tsunashima, H. "Railway Condition Monitoring, Present and Application for Regional Railways", presented at Conference of the Transportation and Logistics Sector Meeting, Tokyo, Japan, Dec. 4–6, 2017. https://doi.org/10.1299/jsmetld.2017.26.CL

[5] Azzoug, A., Kaewunruen, S. "RideComfort: A Development of Crowdsourcing Smartphones in Measuring Train Ride Quality", Frontiers in Built Environment, 3, 3, 2017. https://doi.org/10.3389/fbuil.2017.00003

[6] Paixão, A., Fortunato, E., Calçada, R. "Smartphone's Sensing Capabilities for On-Board Railway Track Monitoring: Structural Performance and Geometrical Degradation Assessment", Advances in Civil Engineering, 2019, 1729153, 2019. https://doi.org/10.1155/2019/1729153

[7] Cong, J., Gao, M., Wang, Y., Chen, R., Wang, P. "Subway rail transit monitoring by built-in sensor platform of smartphone", Frontiers of Information Technology & Electronic Engineering, 21(8), pp. 1226–1238. 2020. https://doi.org/10.1631/FITEE.1900242

[8] Rodríguez, A., Sañudo, R., Mirabda, M., Gómez, A., Benavente, J. "Smartphones and tablets applications in railways, ride comfort and track quality. Transition zones analysis", Measurement, 182, 109644, 2021. https://doi.org/10.1016/j.measurement.2021.109644

[9] NeTIRail-INFRA "D4.6. - Low cost smartphone based track and ride quality monitoring technology", [pdf] Needs Tailored Interoperable Railway Infrastructure, Sheffield, UK, 2017. Available at: https://ec.europa.eu/research/participants/documents/downloadPublic?documentIds=080166e5b4461582&appId=PPGMS

[10] Chia, L., Lu, P., Bhardwaj, B., Bridgelall, R., Tolliver, D., Dhingra, N. "Automatic Rail Track Surface Anomaly Detection with Smartphone Based Monitoring System", In: 2019 International Conference on Informatics, Control and Robotics (ICICR 2019), Shanghai, China, 2019, pp. 168–172. ISBN: 978-1-60595-633-6 https://doi.org/10.12783/dtetr/icicr2019/30565

[11] Do, N. T., Haji Abdulrazagh, P., Gül, M., Hendry, M. T., Roghani, A., Toma, E. "Evaluating Passenger Railway Ride Quality Over Long Distances Using Smartphones", In: 2020 Joint Rail Conference, St. Louis, Missouri, USA, 2020, Paper No JRC2020-8093. ISBN: 978-0-7918-8358-7 https://doi.org/10.1115/JRC2020-8093

[12] Siemens "Track monitoring ensures 100% system availability: Continuous information about track condition with the track monitoring smartphone app", [online] Available at: https://www.mobility.siemens.com/global/en/portfolio/rail/stories/track-monitoring-smartphone-app.html [Accessed: 25 May 2021]

[13] UIC "UIC Harmotrack Project: a worldwide project bringing together companies across five continents", [online] Available at: https://uic.org/com/enews/nr/698/article/uic-harmotrack-project-a-worldwide-project-bringing-together-companies-across?page=modal_enews

[14] Ágh, C. "A new arrangement of accelerometers on track inspection car FMK-007 for evaluating derailment safety", presented at Track Maintenance Machines in Theory and Practice - SETRAS 2018, Žilina, Slovakia, Nov. 7–8, 2018.

[15] Császár, L., Pálfi, C. "Determination of Wheel-Rail Contact Forces Using Different Measurement Methods", presented at 9th International Conference on Railway Bogies and Running Gears, Budapest, Hungary, Sep. 9–12, 2013.

[16] CEN "EN 12299:2009 Railway applications - Ride comfort for passengers - Measurement and evaluation", European Comittee for Standardization, Brussels, Belgium, 2009.

[17] CEN "EN 15273-1:2013 Railway applications. Gauges General. Common rules for infrastructure and rolling stock", European Comittee for Standardization, Brussels, Belgium, 2013

[18] Karaim, M., Elsheikh, M., Noureldin, A. "GNSS Error Sources", In: Rustamov, R. B., Hashimov, A. M. (Eds.) Multifunctional Operation and Application of GPS, IntechOpen, London, UK, 2018. ISBN: 978-1-78923-215-8 https://doi.org/10.5772/intechopen.75493